Study of the Electric Quadrupole Interaction in Antiferroelectric $PbHfO_3$ by Perturbed γ-γ Angular Correlations and Mössbauer Spectroscopy

M. Forker, A. Hammesfahr, A. Lopez-García,* and B. Wolbeck
Institut für Strahlen- und Kernphysik der Universität Bonn, Bonn, Germany
(Received 1 May 1972; revised manuscript received 30 June 1972)

The temperature dependence of the electric quadrupole interaction in polycrystalline antiferroelectric $PbHfO_3$ has been investigated in the temperature range -253 to $+225$ °C by perturbed angular correlations and Mössbauer measurements. Three different phases have been observed with transition temperatures of 163 and 215 °C in agreement with the results of crystal-structure studies. In the two tetragonal phases below 215 °C the compound is known to be antiferroelectric; in the cubic phase above 215 °C it is paraelectric. It has been suggested by Shirane and Pepinsky that the antiferroelectricity of $PbHfO_3$ for temperatures below 163 °C (phase I) is due to the same type of ion displacements which lead to the antiferroelectricity of $PbZrO_3$. The results of our measurements strongly support this suggestion. In both tetragonal phases the observed quadrupole-interaction strength decreases with increasing temperature. For phase I this temperature dependence can be explained qualitatively by the variation of the lattice parameters with temperature, as shown by a lattice-sum calculation.

I. INTRODUCTION

Some dielectrics exhibit phase changes with almost all the characteristics of ferroelectric transitions, such as a maximum of the dielectric constant, discontinuity of the specific heat, and changes in the symmetry and dimensions of the unit cell. They do not show, however, the most prominent properties of ferroelectric compounds: There exists neither a macroscopic spontaneous polarization nor a hysteresis loop. Even before the discovery of such compounds Kittel[1] gave a theoretical treatment of this kind of collective instability. Starting from an analogy with antiferromagnetics, he showed that in crystals with lines of spontaneously polarized ions not only parallel polarization of neighboring lines (ferroelectricity) but also antiparallel polarization (antiferroelectricity) is energetically possible and under certain circumstances favored over the parallel alignment. For the latter case the bulk spontaneous polarization is obviously zero.

Among the first to report experimental evidence for the existence of an antiferroelectric configuration were Sawaguchi, Maniwa, and Hoshino.[2] A careful study of a single crystal of lead zirconate ($PbZrO_3$) revealed the existence of antiparallel lines of spontaneous polarization in this compound.

Most of the data available about antiferroelectrics were obtained by x-ray and neutron-diffraction studies, and measurements of the dielectric constant and the specific heat. These measurements mainly yield information about the crystal structure, antiparallel displacement of certain atoms, phase transitions, and the bulk dielectric properties.

Another quantity of great interest is the internal electric field gradient (EFG) in antiferroelectric compounds. Since the EFG reflects the microscopic charge distribution, its determination and especially the investigation of its temperature dependence should yield valuable information about the mechanism which leads to the antiferroelectricity. So, in recent Mössbauer-effect measurements,[3,4] the EFG in antiferroelectric compounds, such as $PbZrO_3$, was carefully investigated as a function of temperature. In all these cases, however, the compound studied had to be doped considerably with Mössbauer-sensitive isotopes, such as ^{57}Co and ^{119m}Sn. This doping most probably alters the properties of the base material and makes interpretation of the observed internal EFG difficult. It therefore seemed interesting to study the internal EFG in lead hafnate ($PbHfO_3$), which is an antiferroelectric compound with properties close to those of $PbZrO_3$. $PbHfO_3$ can be investigated by angular correlation and Mössbauer-effect measurements without the necessity of doping, since Hf is one of the very few elements that provide isotopes favorable for both techniques.

II. PROPERTIES OF LEAD ZIRCONATE AND LEAD HAFNATE

Since lead zirconcate is one of the best-studied cases[5-8] of antiferroelectricity, and lead hafnate and lead zirconate behave very similarly, we shall shortly discuss the dielectric properties of these compounds. The most characteristic features of lead zirconate, obtained by the study of a single crystal, are as follows.

(a) Lead zirconate belongs to the perovskite family and has two phases with different lattice structures. Below 230 °C the unit cell is pseudotetragonal, with $c/a < 1$; above this temperature it

is cubic.

(b) In the tetragonal phase the dielectric constant increases with temperature to reach a maximum at the Curie temperature of $T_C = 230\,^\circ\mathrm{C}$. In the cubic phase the compound is paraelectric; the dielectric constant decreases with $1/(T - T_C)$.

(c) On application of external electric fields up to 30 kV/cm no hysteresis loop is observed. At higher fields the compound changes from the antiferroelectric to a ferroelectric configuration, giving rise to hysteresis.

(d) An x-ray analysis of the tetragonal phase shows, besides the main lines due to the perovskite structure, some extra, so-called superlattice lines. A careful examination of these lines combined with additional neutron-diffraction studies[8] proves the antiferroelectricity of $PbZrO_3$. The analysis shows that with respect to the ideal perovskite structure Pb atoms suffer antiparallel shifts along the original cubic [110] direction; the oxygen atoms as well suffer antiparallel shifts within the (001) plane and in addition unbalanced antiparallel shifts along the c direction. The numerical values of these shifts are listed in Ref. 8. These antiparallel displacements destroy the simple periodicity of the lattice structure, as can be seen from Fig. 6 of Ref. 8. Periodicity is only regained by combining several unit cells to an orthorhombic supercell. The superlattice created in this way gives rise to additional lines in the x-ray spectrum.

In many aspects $PbHfO_3$ and $PbZrO_3$ behave very similarly. $PbHfO_3$ has been studied as a ceramic by Shirane and Pepinsky.[9] Its essential properties compare to those of lead zirconcate in the following ways.

(a) Lead hafnate, as well, is a member of the perovskite family. There exist, however, three phases with different crystal structures. Phase I (up to 163 °C) is tetragonal, with $c/a < 1$; phase II (163–215 °C) is again tetragonal, with c/a larger than in phase I, but still $c/a < 1$; phase III (above 215 °C) is cubic.

(b) The dielectric constant shows anomalies at the transition temperatures.

(c) There exists no hysteresis loop, even on application of external electric fields up to 60 kV/cm.

(d) The x-ray spectrum of the compound shows weak superlattice lines in both tetragonal phases. The exact structure of the superlattice could not be deduced from these lines. For this purpose the study of a single crystal is necessary. In both phases the superlattice lines are different. For phase I, Shirane and Pepinsky suggest a superstructure equivalent to that of $PbZrO_3$. No neutron-diffraction studies have been performed for $PbHfO_3$ up to now.

These experimental results are evidence for the antiferroelectricity of both tetragonal phases of $PbHfO_3$. In the cubic phase the compound is paraelectric.

III. ANGULAR CORRELATION MEASUREMENTS

A. General Theory

Perturbed angular correlation measurements provide a powerful tool for the investigation of internal fields, their dispersion and time dependence. The possibility of using nuclei as a microscopic field-sensitive probe is due to the fact that the angular correlation of two successive γ rays can be perturbed by the hyperfine interaction between the nuclear moments of the intermediate state of the cascade and electromagnetic fields acting on the nucleus.

The theory of perturbed angular correlations is well developed.[10] The unperturbed angular distribution has the form

$$W(\theta) = 1 + A_2 P_2(\cos\theta) + A_4 P_4(\cos\theta) \,. \tag{1}$$

Perturbations have the effect that the coefficients of the Legendre polynomials become time dependent. The time dependence can be expressed by including the perturbation factors $G_{kk}(t)$:

$$W(\theta, t) = 1 + A_2 G_{22}(t) P_2(\cos\theta) + A_4 G_{44}(t) P_4(\cos\theta). \tag{2}$$

In the following we shall restrict the discussion to static quadrupole interactions for the spin $I = \frac{5}{2}$, which is the case of interest in this paper.

The EFG tensor which interacts with the nuclear quadrupole moment can be characterized by its maximal component V_{zz} and the asymmetry parameter η:

$$\eta = (V_{yy} - V_{xx})/V_{zz} \,, \tag{3}$$

where the principal axes are chosen in such a way that

$$|V_{yy}| \leq |V_{xx}| \leq |V_{zz}| \,.$$

The EFG splits a level with $I = \frac{5}{2}$ into three states, whose energies depend on the asymmetry parameter. To the three possible transitions between these states correspond frequencies ω_1, ω_2, and ω_3 which depend on η, but always fulfill the condition

$$\omega_1 + \omega_2 = \omega_3 \,.$$

Consequently the asymmetry parameter η can be written as a function of the ratio ω_2/ω_1. In Ref. 11 the relation between these two quantities is given for spin $I = \frac{5}{2}$. ω_1 is related to the quadrupole frequency ω_Q for $\eta = 0$ by

$$\omega_1 = 3\omega_Q \quad \text{for } I \text{ integer}$$

$$= 6\omega_Q \quad \text{for } I \text{ half-integer} \,,$$

where ω_Q is defined as

$$\omega_Q = \frac{e^2 V_{zz} Q}{4I(2I-1)} \quad . \tag{4}$$

The perturbation factor $G_{kk}(t)$, which describes the modulation of the angular correlation by the hyperfine interaction as a function of time can be evaluated in terms of the frequencies ω_n. For static interactions, oriented randomly in space, it takes the form

$$G_{kk}(t) = \sigma_{k0} + \sum_{n=1}^{3} \sigma_{kn} \cos\omega_n t \ . \tag{5}$$

For a given spin I, the amplitudes σ_{kn} are functions only of the asymmetry parameter η. Their calculations are described in detail in Ref. 12. For $I = \frac{5}{2}$ they are listed in Ref. 11. So the perturbation factor $G_{kk}(t)$ contains only two linear independent quantities, ω_Q and η. Consequently a measurement of $G_{kk}(t)$ yields information about the strength of the interaction (ω_Q) and its symmetry (η).

Owing to lattice imperfections and impurity centers, it is frequently observed that the EFG is not exactly the same at all lattice sites, so that the frequencies ω_n are not sharply defined, but distributed with some relative width about a mean value. Such frequency distributions, of course, will influence the perturbation factor. Supposing a normal shape with relative width δ for this frequency distribution, the perturbation factor has to be written as[11]

$$G_{kk}(t) = \sigma_{k0} + \sum_{n=1}^{3} \sigma_{kn} e^{-\delta^2\omega_n^2 t^2/2} \cos\omega_n t \ . \tag{6}$$

For a Lorentzian distribution with width Λ one obtains

$$G_{kk}(t) = \sigma_{k0} + \sum_{n=1}^{3} \sigma_{kn} e^{-\Lambda\omega_n t} \cos\omega_n t \ . \tag{7}$$

B. Source Preparation

The 133–482-keV γ-γ cascade of the 45-day isotope ^{181}Hf, which decays to ^{181}Ta, is one of the most favorable cases for time-differential angular correlation measurements. The lifetime of the 482-keV state is $T_{1/2} = 10.95$ nsec, its spin $I = \frac{5}{2}$, and the A_2 coefficient of the cascade $A_2 \approx -0.25$, so that the experimental situation is relatively easy to handle.

The radioactivity is obtained by the reaction ^{180}Hf$(n, \gamma)^{181}$Hf. For the preparation of $PbHfO_3$ we followed more or less the method applied by Shirane and Pepinsky.[9] Radioactive HfO_2 and reagent-grade PbO were mixed well in equimolar proportions, pressed to a pellet, and sintered. We encountered, however, difficulties using the sintering temperature of 1200 °C as applied by the authors of Ref. 9. The specimen prepared at this temperature contained considerable amounts of HfO_2, which had not undergone a reaction, as was shown by the existence of HfO_2 lines in the x-ray spectrum of the probe. This is very probably due to the high volatility of PbO.

By preparation of various compounds at different temperatures it turned out that by decreasing the sintering temperature and increasing the sintering time this difficulty can be avoided. So the specimen sintered at 850 °C for 36 h and was free of HfO_2 contribution.

C. Equipment

The time-differential measurements were performed with a four-detector angular correlation apparatus which is described in detail in Ref. 13. This apparatus is designed in such a way that it yields simultaneously four independent time-differential measurements of the same angular correlation. The time resolution obtained for the energies of the relevant cascade varied between 2.2 and 2.5 nsec full width at half-maximum (FWHM) for the four different combinations.

The source temperature was varied in the range −196 to +22 °C by means of commercial cryostat. For source temperatures above +22 °C a heating system was designed which yielded a stability of approximately 1 °C for the source temperature.

D. Perturbed Angular Correlation Measurements, Data Treatment, and Results

The measurements were performed at 15 different source temperatures from −196 to +225 °C. From the time spectra of the coincidences observed at the three angles 90°, 135°, and 180° the coefficients $A_2G_{22}(t)$ were determined in the conventional way for each of the four detector combinations. Figures 1–3 show as examples the time spectra obtained with one combination at −42, 203.5, and 218 °C.

We derived the interaction frequencies in first approximation by a Fourier analysis of the observed spin-rotation curves. For an accurate determination of these frequencies and the other parameters describing the perturbation the least-squares-fit technique is more suitable for the type of spectra investigated here.[14]

For temperatures below 163 °C the measured perturbation factors exhibit clearly a periodic but slightly damped structure (see Fig. 1). Here the frequencies contributing to the perturbation are easily obtained by a fit of Eq. (6) or (7) to the experimental data. It cannot, however, be decided from the fits whether the observed damping of the amplitudes is caused by a normal-shaped or Lorentzian-shaped frequency distribution. Only the existence of a distinct second lattice site can be excluded for temperatures below 163 °C.

The solid lines in Figs. 1 and 2 are the result

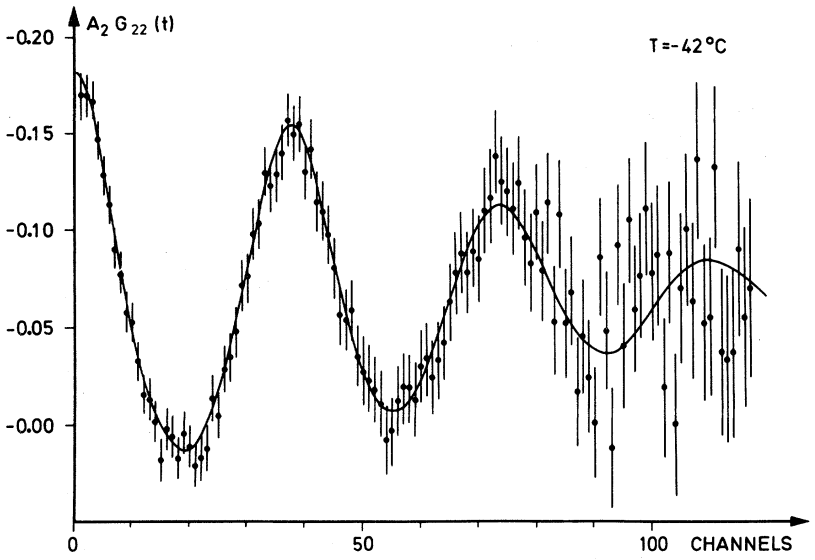

FIG. 1. Perturbed angular correlation of ^{181}Ta in $PbHfO_3$ at $-42\,^{\circ}C$. Calibration: 328 psec/channel.

of a least-squares fit assuming a normal-shaped frequency distribution. The finite time resolution of the equipment has been taken into account by numerical convolution with the time-response curve. Each of the four combinations was treated separately in this way. The final values of the parameters given in Table I are obtained by averaging the results of the four combinations.

Table I contains the values ω_1, η, and δ as derived from the fits. From ω_1 and the asymmetry parameter η the quadrupole frequency ω_Q has been determined and is included in Table I, as well as the EFG V_{zz} which has been evaluated from the quadrupole frequency ω_Q using for the quadrupole moment of the 482-keV state of ^{181}Ta the value[15]

$$Q(482\ \text{keV}) = (2.53 \pm 0.10) \times 10^{-24}\ \text{cm}^2 .$$

For temperatures between 163 and 215 °C the observed time spectra no longer exhibit a periodic structure. An extremely strong damping of the oscillation amplitudes occurs in this temperature range, as illustrated by Fig. 2. Analysis of this kind of time spectra is very difficult because of the complete loss of any oscillatory character. We have tried several approaches for the evaluation of these time spectra. First, a sum of cosine terms

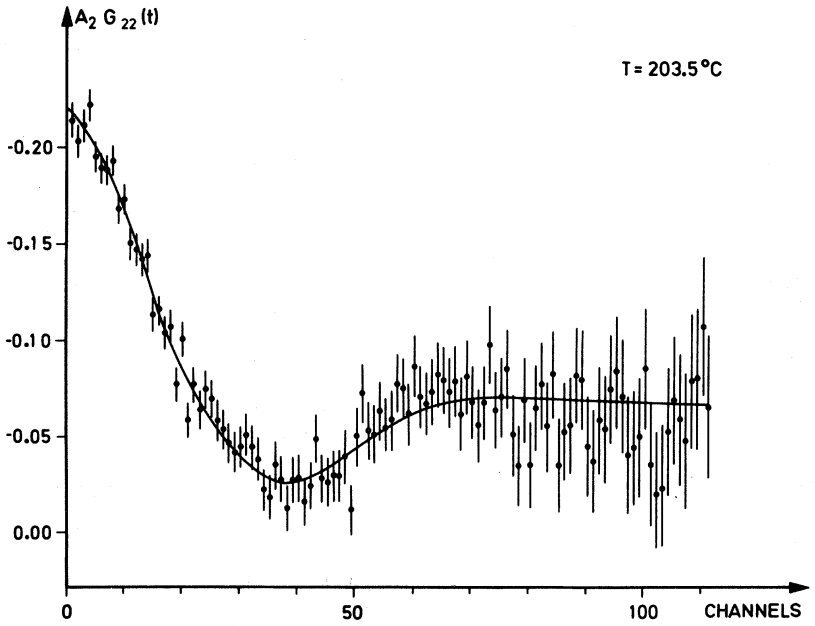

FIG. 2. Perturbed angular correlation of ^{181}Ta in $PbHfO_3$ at 203.5 °C. Calibration: 337 psec/channel.

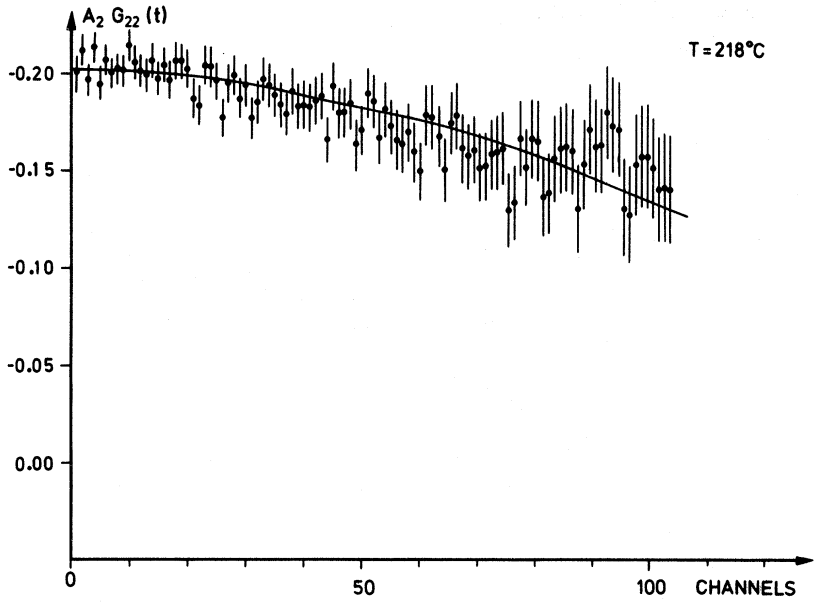

FIG. 3. Perturbed angular correlation of ^{181}Ta in $PbHfO_3$ at 218 °C. Calibration: 337 psec/channel.

like Eq. (6) or (7) was fitted to the experimental points. From these fits we obtained values for ω_1, η, and the frequency distribution δ. No distinction was possible between a normal-shaped and Lorentzian-shaped distribution. In a further attempt we allowed for a second distinct lattice site. This procedure yielded fits comparable to those of the first approach. The frequency obtained in this way for the first lattice site did not change; the frequency distribution, however, decreased by approximately 50%. The frequencies obtained for the second lattice site were in the order of 20% of those of the first lattice site. The statistical accuracy of the measurements does not permit a decision as to which of the two approaches is the better one.

It can be excluded that the observed damping in this phase is due to a relaxation mechanism. In case of relaxation the perturbed angular correlation would decrease continuously towards zero, whereas the observed time spectra maintain the hard-core value at large delay times.

The values of ω_1, η, and δ given in Table I were obtained from the fits on the assumption of a single lattice site.

In the cubic phase above 215 °C no quadrupole interaction should be present. A small remaining interaction, however, is observed above the Curie point. We attribute this interaction to imperfections of the lattice structure (see Fig. 3).

It should be mentioned that in the presence of a field dispersion the determination of the asymmetry of the crystal structure is problematic. It

TABLE I. Experimental results for $PbHfO_3$.

T (°C)	ω_1 (Mc/sec)	η	ω_Q (Mc/sec)	$\lvert V_{zz}\rvert$ (10^{17} V/cm^2)	δ (%)
−196.0	539.7 ± 6.2	0.87 ± 0.02	54.97 ± 1.65	5.79 ± 0.17	7.4 ± 0.6
−100.0	519.3 ± 4.3	0.87 ± 0.02	52.90 ± 1.30	5.57 ± 0.14	7.0 ± 0.6
−42.0	498.9 ± 4.9	0.87 ± 0.02	50.82 ± 1.27	5.35 ± 0.13	7.5 ± 0.5
+22.0	435.4 ± 3.4	0.80 ± 0.02	46.80 ± 0.45	4.93 ± 0.10	7.0 ± 0.6
+65.0	411.1 ± 3.0	0.78 ± 0.02	45.02 ± 1.20	4.74 ± 0.13	6.3 ± 0.7
+120.5	361.3 ± 3.3	0.76 ± 0.02	40.17 ± 1.12	4.23 ± 0.12	7.7 ± 0.7
+152.0	306.0 ± 3.8	0.68 ± 0.02	36.32 ± 1.15	3.83 ± 0.12	7.2 ± 0.7
+169.0	238.6 ± 6.2	0.68 ± 0.09	28.03 ± 2.23	2.95 ± 0.24	26.3 ± 2.8
+175.0	198.1 ± 4.2	0.68 ± 0.09	23.28 ± 1.82	2.45 ± 0.19	42.3 ± 4.0
+188.5	181.7 ± 4.8	0.60 ± 0.10	22.72 ± 1.81	2.39 ± 0.19	42.8 ± 4.0
+203.5	172.6 ± 3.6	0.61 ± 0.09	21.42 ± 1.67	2.26 ± 0.18	44.8 ± 4.9
+208.0	139.7 ± 2.5	0.48 ± 0.09	19.10 ± 1.47	2.01 ± 0.15	41.8 ± 3.9
+211.0	137.8 ± 2.5	0.52 ± 0.09	18.18 ± 1.40	1.92 ± 0.15	41.4 ± 4.3
+218.0	21.1 ± 6.6		3.52 ± 1.10	0.37 ± 0.12	
+225.0	17.5 ± 6.1		2.92 ± 1.02	0.30 ± 0.12	

is of course possible to calculate an asymmetry parameter from the experimentally determined frequencies ω_1 and ω_2. But for the case of a large field distribution this value does not necessarily permit a conclusion about the asymmetry of the perfect crystal.

In a perfect crystal the interaction frequencies are the same for all unit cells. If lattice imperfections are present, the interaction frequencies will vary from microcrystal to microcrystal, giving rise to frequency distributions. The variation of the frequencies might be such that the ratio ω_2/ω_1 is the same in all unit cells. In this case the asymmetry parameter would coincide with that of the perfect crystal. In general, however, also the ratio ω_2/ω_1 and consequently the asymmetry parameter will vary for different microcrystals. The results will be a distribution of the asymmetry parameter, and the mean value of this distribution will in general not coincide with the asymmetry parameter of the perfect crystal. This can be seen best for the case where the asymmetry parameter of the perfect crystal is zero. Since η is confined to the range 0–1, the distribution of η will have a mean value different from zero, and this value will be the larger the larger the field dispersion. For a perfect crystal with $\eta = 1$, lattice imperfections will accordingly produce a distribution of the asymmetry parameter, the mean value of which is less than 1, and the smaller it is, the larger the field dispersion. For these reasons it is difficult to deduce from a measured ratio ω_2/ω_1 the asymmetry parameter of a crystal structure which is subject to strong lattice imperfections.

In phase II of $PbHfO_3$ the frequency distribution is extremely large, so that here the difficulties just discussed arise. To allow for the uncertainty of the asymmetry parameter caused by the field dispersion we therefore increased the statistical errors of the asymmetry parameter in phase II by a factor of 2. This, of course, leads to relatively large errors for the quadrupole frequency and the EFG.

In Fig. 4 the quadrupole frequency ω_Q is displayed as a function of temperature.

E. Discussion of Perturbed Angular Correlation Results

The quadrupole frequency ω_Q as displayed in Fig. 4 exhibits clearly discontinuities at the two transition temperatures 163 and 215 °C. In both tetragonal phases the frequency ω_Q decreases with increasing temperature. For phase I this might be expected from the temperature dependence of the lattice parameters c and a; for phase II one would expect accordingly a more or less constant interaction frequency.[9]

To obtain more detailed information on how the EFG at the nuclear site depends on the lattice parameters, a lattice-sum calculation was performed for a point-charge tetragonal lattice with the lattice parameters c and a from Ref. 9 at various temperatures. The calculation was extended over ten unit cells in each direction.

To compare these calculated values of the EFG with those obtained by the experiment the Sternheimer correction $1-\gamma_\infty$ has to be taken into account. We took $1-\gamma_\infty = 62.2$ for Ta^{5+} from the tabulation of Feiock and Johnson.[16] The values of $(1-\gamma_\infty)\cdot V_{zz}$ calculated in this way are smaller than the experimental values by approximately a factor of 2. This, of course, is due to the fact that the point-charge model is only a very rough approximation of the real situation, since it does not take into account the dipole moments induced in the ligands nor deviations of the ideal tetragonal structure due to the antiferroelectricity of the compound, nor the covalent character of the bonds. From chemical shift measurements[17] it is known that the bonds in $PbHfO_3$ are not of a pure ionic character. A considerable covalent contribution is present[18] which is not temperature dependent.

It should, however, be possible to compare the qualitative temperature dependence of the calculated and the measured EFG. For this purpose the ratio $V_{zz}(T)/V_{zz}(65\,^\circ\mathrm{C})$ was calculated which describes

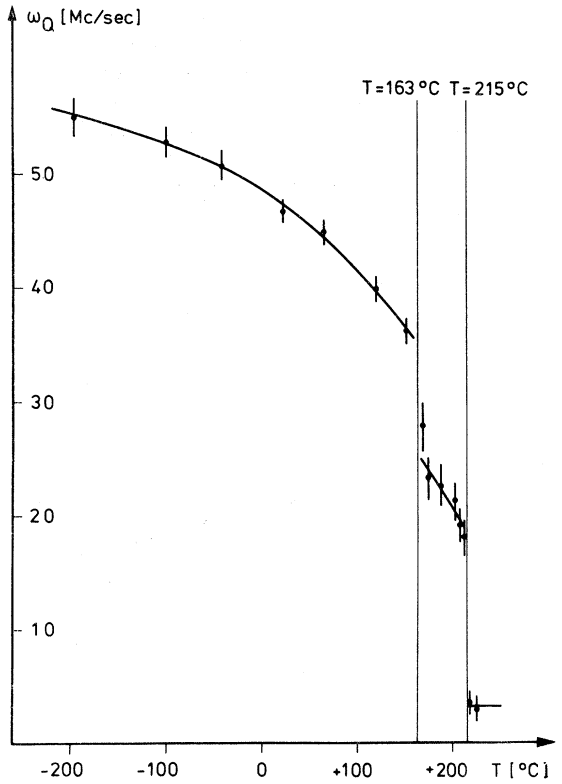

FIG. 4. Interaction frequency ω_Q as a function of temperature.

the relative change for both the calculated and the experimental values. The result is plotted in Fig. 5. The large errors of the experimental values of the EFG in phase II are due to the uncertainty of the asymmetry parameter. It can be seen that in phase I the relative temperature dependence of the calculated and measured EFG agree fairly well, so that, in fact, the observed change of the EFG can be attributed mainly to the change of the lattice parameters.

For phase II the calculation yields a nearly constant EFG, in contradiction to the experimental observation. The measured relative EFG is larger than the calculated value and decreases more strongly with temperature than the model calculation predicts. This decrease of the EFG with temperature in phase II might be due to a decrease of the antiferroelectric distortion of the tetragonal lattice as temperature approaches the Curie point.

From the x-ray analysis of ceramic $PbHfO_3$ Shirane and Pepinsky[9] suggest that the antiferroelectricity in phase I of $PbHfO_3$ is of the same type as encountered in $PbZrO_3$. This suggestion is based on the similarity of the superstructure lines observed in $PbHfO_3$ and $PbZrO_3$. Our experimental results are in agreement with this proposal. The environment of the Zr site in the multiple unit cell of $PbZrO_3$ is axially nonsymmetric. We have calculated the EFG tensor of this site from a point-charge model, using the values of the ion displacements at room temperature as given in Ref. 8. From the components of the EFG tensor the asymmetry parameter can be deduced. The calculation yields an asymmetry parameter of 0.85 for the Zr site in $PbZrO_3$ at room temperature.

The experimentally determined asymmetry parameter of $PbHfO_3$ (see Table I) at room temperature is in very good agreement with the result of the calculation, thus strongly supporting the conclusion of Shirane and Pepinsky[9] that the antiferroelectricity in phase I of $PbHfO_3$ is due to the same type of ion displacement as found in $PbZrO_3$. It is interesting to note that the measured asymmetry parameter (see Table I) decreases with increasing temperature, indicating a decrease of the antiferroelectric distortion of the unit cell.

In both tetragonal phases the spin-rotation patterns are damped. In phase I the damping is relatively weak; in phase II it is so pronounced that any oscillation is lost. The observed rapid change of the damping between phases I and II is quite a remarkable fact. Usually a damping of spin-rotation patterns observed in solid environments is attributed to a frequency distribution caused by lattice imperfections. Our data indicate that after the transition from phase I to phase II the amount of lattice imperfections is drastically increased. In this connection it should be mentioned that after lowering the temperature from phase II to phase I the spin-rotation curves observed in this phase before were reproduced.

An explanation of this experimental result has not yet been found. It seems possible that the strong damping in phase II is connected with the existence of a temperature-dependent transverse-optical lattice mode in $PbHfO_3$. It was shown experimentally for $SrTiO_3$,[19] $BaTiO_3$,[20] and $PbZrO_3$ [3,4] and discussed theoretically by Cochran[21] that close to the Curie point of ferro- and antiferroelectric compounds the transverse optical mode is strongly temperature dependent, the frequencies being rapidly reduced near the Curie point. This leads

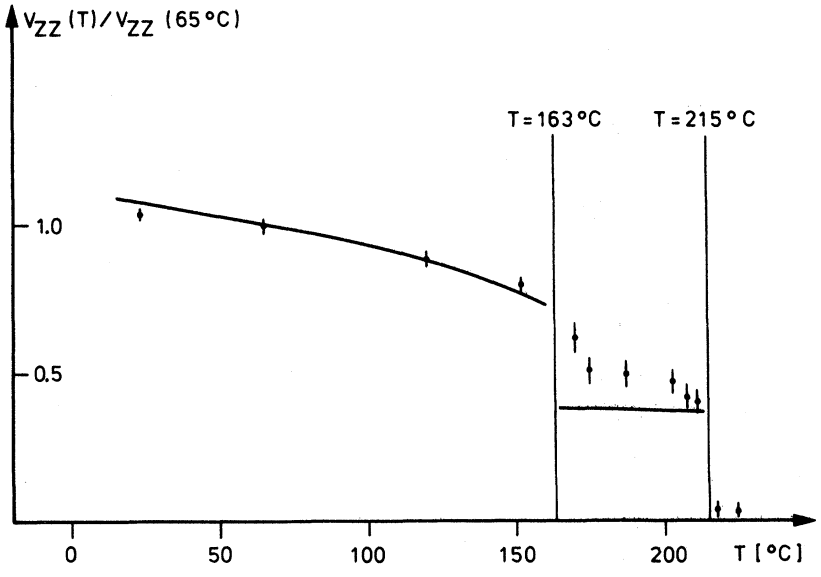

FIG. 5. Comparison of the measured and the calculated values of the electric field gradient for $PbHfO_3$. The solid line represents the EFG calculated from the known lattice parameters by a lattice-sum calculation.

to a softening of the lattice and might increase the tendency for the creation of lattice imperfections.

Our data, however, are not yet sufficient to decide whether our experimental observation can be explained on this basis. Further experiments are necessary which are presently being prepared. In particular, we plan a measurement of the Mössbauer fraction in $PbHfO_3$ as a function of temperature near the Curie point which should yield valuable information about the temperature dependence of the optical mode in this compound and thus possibly contribute to an understanding of the mechanism which leads to the observed strong damping in phase II.

IV. MOSSBAUER MEASUREMENTS

In the angular correlation measurements described in Sec. III we determined the EFG acting on the nucleus of the impurity Ta at the Hf site in $PbHfO_3$. The EFG experienced by the nuclei of the Hf ions in this compound might differ appreciably from that acting on the Ta nuclei. It was discussed earlier that there is a considerable contribution to the EFG due to the covalent character of the bonds in $PbHfO_3$. This contribution will depend on the charge state of the central ion. The charge of the Hf ions in $PbHfO_3$ is 4+, that of the Ta ions most probably 5+, and consequently a difference of the EFGs experienced by the nuclei of the two ions is to be expected. For compounds like HfO_2 and $(NH_4)_2HfF_6$ this difference has been found to be on the order of 10%.[15]

We found it interesting to study this difference as well for the case of $PbHfO_3$. For this purpose the EFG acting on the Hf nuclei in $PbHfO_3$ was determined by a Mössbauer experiment, using the 93-keV transition of ^{178}Hf as the source and inactive $PbHfO_3$ as an absorber. The ^{178}Hf activity was obtained by irradiation of a Ta foil with 40-MeV deuterons: $^{181}Ta\ (d, 5n)^{178}Hf$. The 93-keV Mössbauer transition of this source showed essentially no line broadening. The preparation of the absorber material has been described above.

The electric hyperfine interaction was observed at the temperatures of liquid hydrogen and liquid nitrogen. Figure 6 shows the Mössbauer spectrum taken at liquid-hydrogen temperature. The solid line is the result of a least-squares fit which has been performed following standard techniques.

From the hyperfine splitting, as derived from the fit, the EFG acting on the Hf nuclei in $PbHfO_3$ can be determined. Using for the quadrupole moment of the 93-keV level of ^{178}Hf the value[22]

$$Q(93\ \text{keV}) = -1.95\times10^{-24}\ \text{cm}^2\ ,$$

the calculation yields

$$V_{zz} = -(6.10\pm1.21)\times10^{+17}\ \text{V/cm}^2 \text{ at } T = -253\ ^\circ\text{C}$$

$$= -(5.19\pm1.30)\times10^{+17}\ \text{V/cm}^2 \text{ at } T = -196\ ^\circ\text{C}.$$

The asymmetry parameter of the interaction could not be determined, since the fit was not sensitive enough to this quantity. The negative sign of the EFG deduced from the Mössbauer spectra agrees with the result of the calculated lattice sum dis-

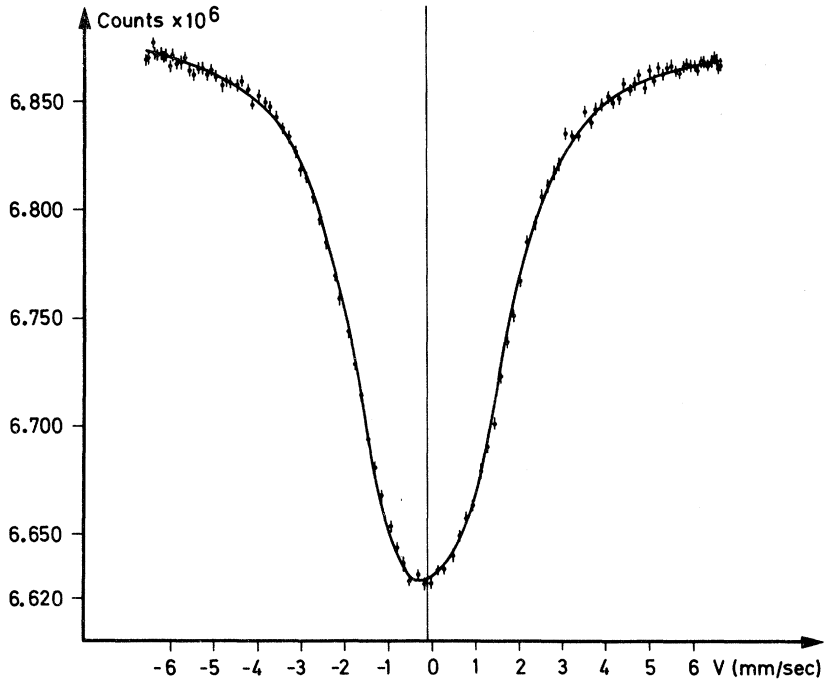

FIG. 6. Mössbauer absorption spectrum of $PbHfO_3$ at liquid-hydrogen temperature.

cussed above.

In the temperature range covered by the experiment the EFG increases slightly with decreasing temperature, in agreement with the behavior observed at higher temperatures by the angular correlation measurements. At $-196\,^{\circ}C$ the EFG acting on the Hf nuclei in $PbHfO_3$ is approximately 10% smaller than that acting on the Ta nuclei (see Table I). This difference is of the same size as found in HfO_2 and $(NH_4)_2HfF_6$.

ACKNOWLEDGMENTS

The authors are indebted to Professor E. Bodenstedt for his kind interest and support of this work. The generous support by the Bundesministerium für Bildung und Wissenschaft is gratefully acknowledged. The numerical calculations have been performed on the IBM 370 computer of the Rheinisch-Westfälisches Institute für Instrumentelle Mathematik.

*Fellow from Consejo Nacional de Investigaciones Cientificas y Tecnicas, Buenos Aires, Argentina.

[1]C. Kittel, Phys. Rev. 82, 729 (1951).

[2]E. Sawaguchi, A. Maniwa, and B. Hoshino, Phys. Rev. 83, 1078 (1951).

[3]A. P. Jain, S. N. Shringi, and L. M. Sharma, Phys. Rev. B 2, 2756 (1970).

[4]J. P. Canner, C. M. Yagvik, R. Gerson, and W. J. James, J. Appl. Phys. 42, 4708 (1971).

[5]G. Shirane, Phys. Rev. 86, 219 (1952).

[6]G. Shirane, E. Sawaguchi, and Y. Takagi, Phys. Rev. 84, 476 (1951).

[7]E. Sawaguchi, J. Phys. Soc. Japan 8, 615 (1953).

[8]F. Jona, G. Shirane, F. Mazzi, and R. Pepinsky, Phys. Rev. 105, 849 (1957).

[9]G. Shirane and R. Pepinsky, Phys. Rev. 91, 812 (1953).

[10]H. Frauenfelder and A. Steffen, in *Perturbed Angular Correlations*, edited by K. Karlsson, E. Matthias, and K. Siegbahn (North-Holland, Amsterdam, 1963).

[11]R. Béraud, I. Berkes, J. Danière, G. Marest, and R. Rouguy, Nucl. Instr. Methods 69, 41 (1969).

[12]K. Alder, E. Matthias, B. Olsen, and W. Schneider, in Ref. 10, p. 247.

[13]H. F. Wagner and M. Forker, Nucl. Instr. Methods 69, 197 (1969).

[14]M. Forker and J. D. Rogers, Nucl. Instr. Methods 96, 453 (1971).

[15]E. Gerdau, J. Wolf, H. Winkler, and J. Braunsfurth, Proc. Roy. Soc. (London) A311, 197 (1969).

[16]F. D. Feiock and W. R. Johnson, Phys. Rev. 187, 39 (1969).

[17]D. H. Anderson, J. Chem. Phys. 40, 1168 (1964).

[18]P. da R. Andrade, M. Forker, J. D. Rogers, and J. Kunzler, Phys. Rev. B 6, 2560 (1972).

[19]R. A. Cowley, Phys. Rev. 143, A981 (1964).

[20]V. G. Bhide and M. S. Multani, Phys. Rev. 139, 1983 (1965).

[21]W. Cochran, in *Advances in Physics*, edited by N. F. Mott (Taylor and Francis, London, 1960), Vol. 9, p. 387.

[22]Stelson and Grodzins, Nucl. Data Table A1, 21 (1965).

PHYSICAL REVIEW B VOLUME 7, NUMBER 3 1 FEBRUARY 1973

Compton Profile of Single-Crystal Vanadium

Walter C. Phillips*

Physics Department, Brandeis University, Waltham, Massachusetts 02154

(Received 26 June 1972)

The Compton profile of single-crystal vanadium has been measured with Mo $K\alpha$ x rays. The observed profile shows that the V band electrons are more spatially extended than the density calculated from Hartree–Fock V $3d$ functions. The measured anisotropy in the profile is significantly less than that calculated for free-atom $3d$ functions with an orbital population of 80% t_{2g}.

I. INTRODUCTION

The feasibility of using ~20 keV x rays for accurate single-crystal Compton investigations of $3d$ elements has recently been demonstrated for Fe by Phillips and Weiss.[1] We report here measurements in V using Mo $K\alpha$ (17.4 keV) x rays. The situation for V is experimentally somewhat more favorable than for Fe, because in V the ratio of elastic/Compton scattering is smaller and the $2s2p$ Compton threshold energies are lower.

We have measured the anisotropy in the Compton profile near $J(0)$ for the [110] zone, and the full profile for three crystal orientations. Our results are substantially in agreement with Compton measurements for polycrystalline V at 60 keV made using a Ge-Li detector and recently published by Paakari, Manninen, Inkinen, and Liukkonen.[2] The anisotropy we observe at $J(0)$ is smaller than predicted by earlier x-ray-diffraction measurements[3] of paired reflections in V, and corresponds to a nearly spherical $3d$ momentum (charge) density.